TOPICAL REVIEW — SYNERGETIC EXTREME CONDITION USER FACILITY: BREAKTHROUGHS AND OPPORTUNITIES FOR THE RESEARCH OF PHYSICAL SCIENCE

Attosecond laser station

TOPICAL REVIEW — Synergetic Extreme Condition User Facility: Breakthroughs and opportunities for the research of physical science

Attosecond laser station*

Hao Teng(滕浩)[1], Xin-Kui He(贺新奎)[1], Kun Zhao(赵昆)[1], and Zhi-Yi Wei(魏志义)[1,2,†]

[1] *Beijing National Laboratory for Condensed Matter Physics, Institute of Physics, Chinese Academy of Sciences, Beijing* 100190, *China*
[2] *School of Physical Science, University of Chinese Academy of Sciences, Beijing* 100049, *China*

(Received 18 February 2018; revised manuscript received 4 May 2018; published online 1 June 2018)

The attosecond laser station (ALS) at the Synergetic Extreme Condition User Facility (SECUF) is a sophisticated and user-friendly platform for the investigation of the electron dynamics in atoms, molecules, and condensed matter on timescales ranging from tens of femtoseconds to tens of attoseconds. Short and tunable coherent extreme-ultraviolet (XUV) light sources based on high-order harmonic generation in atomic gases are being developed to drive a variety of end-stations for inspecting and controlling ultrafast electron dynamics in real time. The combination of such light sources and end-stations offers a route to investigate fundamental physical processes in atoms, molecules, and condensed matter. The ALS consists of four beamlines, each containing a light source designed specifically for application experiments that will be performed in its own end-station. The first beamline will produce broadband XUV light for attosecond photoelectron spectroscopy and attosecond transient absorption spectroscopy. It is also capable of performing attosecond streaking to characterize isolated attosecond pulses and will allow studies on the electron dynamics in atoms, moleculars, and condensed matter. The second XUV beamline will produce narrowband femtosecond XUV pulses for time-resolved and angle-resolved photoelectron spectroscopy, to study the electronic dynamics on the timescale of fundamental correlations and interactions in solids, especially in superconductors and topological insulators. The third beamline will produce broadband XUV pulses for attosecond coincidence spectroscopy in a cold-target recoil-ion momentum spectrometer, to study the ultrafast dynamics and reactions in atomic and molecular systems. The last beamline produces broadband attosecond XUV pulses designed for time-resolved photoemission electron microscopy, to study the ultrafast dynamics of plasmons in nanostructures and the surfaces of solid materials with high temporal and spatial resolutions simultaneously. The main object of the ALS is to provide domestic and international scientists with unique tools to study fundamental processes in physics, chemistry, biology, and material sciences with ultrafast temporal resolutions on the atomic scale.

Keywords: attosecond, extreme-ultraviolet (XUV) pulse, pump–probe, photoemission spectroscopy

PACS: 42.55.Vc, 42.65.Re, 79.60.–I, 87.15.ht **DOI:** 10.1088/1674-1056/27/7/074203

1. Introduction

The fundamental processes in matter are governed by the electronic and nuclear motions of the constituent atoms. The electronic motions inherent to these systems are extremely fast.[1] In the Bohr model, which describes the electron classically as a point charge but requires electrons to move in orbits of fixed size and energy, the period is estimated to be 152 as for the smallest orbit of a H atom.[2,3] According to the quantum-mechanical description, the electron motion in the ground-state orbital cannot be observed directly. Alternatively, one may observe charge oscillations resulting from the coherent superposition of electronic states. The period of the electronic oscillation is given by $\Delta E \Delta t = 2\pi\hbar$, where ΔE is the energy spacing of the two eigenstates involved. A larger energy separation ΔE yields faster motion of the particle in the superposition state. For chemical bonds and vibrational states of molecules, energy spacing on the order of meV corresponds to a timescale of tens to hundreds of femtoseconds; thus, typical femtosecond laser pulses may resolve the dynamical processes of molecules.[4] For strongly correlated electrons in a superconductor, hot electrons moving collectively in high-density plasma, electrons on inner shells of atoms or molecules, or electrons bonded in semiconductor nanostructures, the energy spacing between eigenstates ranges from sub-eV to tens of eV; thus, the electrons move significantly faster, and the corresponding timescale is reduced to the attosecond level. For example, the oscillation period of valence electron wave packets in bound atomic or molecular systems is naturally on the order of 100 as.[5]

At the dawn of the 21st century, isolated coherent attosecond extreme-ultraviolet (XUV) pulses were produced; thus, the timescale steered by humans was increased from femtoseconds to attoseconds.[6] This not only introduced new levels for the laser pulse duration and temporal resolution but also, coupled with pump–probe spectroscopy, was a significant step for scientists to master a new and powerful tool to investigate ultrafast processes inside atoms and molecules with unprece-

*Project supported by the National Key R&D Program of China (Grant Nos. 2018YFB1107200, 2017YFC0110301, and 2017YFB0405202), Strategic Priority Research Program of the Chinese Academy of Sciences (Grant No. XDB0703030), and the National Natural Science Foundation of China (Grant Nos. 11474002, 11674386, 61575219, and 61690221).

†Corresponding author. E-mail: zywei@iphy.ac.cn

dented precision. Attosecond XUV pulses have been and will continue to trigger major revolutions in fundamental physical research, and already introduced new field and research direction — attosecond physics.[7]

In experiments, an isolated attosecond XUV pulse is generated via high-order harmonic generation (HHG) from atoms exposed to intense laser pulses.[8] With the demonstration of the first isolated attosecond pulse (IAP) in 2001,[9] many schemes for IAP generation have been developed, and shorter pulses with higher flux have been demonstrated.[10,11] The first scheme is the amplitude-gating (AG) technique,[12] which selects a continuous spectrum in the cutoff region of high-order harmonics generated by carrier-envelope phase (CEP)-stabilized femtosecond few-cycle laser pulses, and IAPs as short as 80-as were obtained.[13] The second approach is polarization gating (PG),[14] which creates a pulse with time-varying polarization sweeping from circular to linear and then back to circular, yielding a very short window for the generation of a single attosecond pulse. Nisoli group developed this technique to produce short 130-as pulses using CEP-stabilized 5-fs laser pulses,[15] and they also developed above-saturation few-cycle laser fields to generate high energy sub-160-as IAPs.[16] The third method is ionization gating (IG), which provides temporal gating via phase mismatching between the fundamental and harmonic fields. By using this method, 430-as pulses were generated.[17] Double optical gating (DOG)[18] and generalized double optical gating (GDOG),[19] which combine polarization gating with two-color gating (TC), were also developed. This scheme relaxes the requirement on the pulse duration to 28 fs, making it easier to generate IAPs, and is scalable to high energy IAPs. A far broader continuous XUV spectrum covering both plateau and cutoff regions of HHG was generated, and 67-as pulses were demonstrated using a DOG with 7-fs driving laser pulses.[20] Because tilting the wavefront of the driving laser pulses continuously changes the direction of HHG, the harmonic radiation in each half-cycle of the driving pulse can be spatially separated in the far-field and corresponds to a series of IAPs, which is known as spatial gating or an attosecond lighthouse.[21,22] The results above were obtained using a near-infrared (NIR) Ti:sapphire laser at 800 nm. When longer-wavelength lasers at the infrared (IR) or mid-IR bands are adopted as the driving lasers, the HHG is shifted to a shorter wavelength,[23,24] and significantly shorter attosecond pulses can be obtained. Last year, the generation of single attosecond pulses with a duration of 53-as in a spectral range covering the C K-edge in the water window was achieved by Chang group at the University of Central Florida,[25,26] using the polarization gating method driven by a 11.4-fs laser at 1.7 μm from OPCPA pumped by a high-energy Ti:sapphire laser. Only one month later, IAPs of 43-as generated by a similar two-cycle mid-IR laser were demonstrated by Wörner group in ETH Zürich, Switzerland,[27] setting a new world record for the shortest coherent optical pulse. Table 1 lists typical isolated attosecond light sources.

Table 1. Typical single isolated attosecond light sources.

Measured duration/as	Central energy/ bandwidth/eV	Energy	Method	Lab/country	Ref.
67	100/170	unspecified	DOG	UCF/USA	[20]
80	83/28	0.5 nJ	AG	MPQ/Germany	[13]
155	25/8	9 nJ	IG	CNR–IFN/Italy	[16]
130	100/22	70 pJ	PG	CNR–IFN/Italy	[15]
160	83/15	∼ 1 nJ	AG	IOP/China	[113]
53	150/200	unspecified	PG	UCF/USA	[25]
43	120/100	unspecified	AG	ETHZ/Switzerland	[27]
500	25/15	1.3 μJ	TC	RIKEN/Japan	[28]
310	38/40	unspecified	lighthouse	NRC/Canada	[29]
260	93/8.6	unspecified	AG	IC/UK	[30]

In parallel with the development of attosecond laser sources, remarkable progress in applications using isolated attosecond XUV pulses has been made. Almost all applications in the early stages were based on attosecond streaking spectroscopy and attosecond transient absorption technology. Because of the limitation of the attosecond pulse energy, attosecond pump–probe spectroscopy cannot be realized currently. Alternatively, an attosecond pulse and a femtosecond laser pulse may be combined to perform pump–probe spectroscopy.[31,32] By scanning the delay between the attosecond and femtosecond pulses, attosecond streaking (photoelectron) or a transient absorption spectrogram can be realized. From the streaking spectrogram, the attosecond pulses can be retrieved using the algorithm of the frequency-resolved optical gating for the complete reconstruction of the attosecond burst (FROG-CRAB)[33] or using phase retrieval by omega oscillation filtering (PROOF).[34] The principle of the attosecond streaking spectroscopy or a streaking camera is that the laser-induced energy shift of the photoelectrons results in a unique mapping of the temporal profile of the at-

tosecond pulse into a similar energy distribution of the photoelectrons, so that the streaking trace can completely characterize the attosecond pulse and be applied for attosecond resolved measurement of the electron dynamics in matter.[35] The signal includes the primary photoelectrons and the secondary (Auger or inner-shell) electrons ionized by the incident XUV burst. Probing the primary or secondary electrons using the pump–probe technique allows observation of the atomic excitation and subsequent relaxation processes with attosecond resolution in real time. Milestone experiments for applications of attosecond streaking spectroscopy were performed using atoms and molecules, for example, the probing of the inner-shell relaxation dynamics,[39] the delay of the photoemission,[40] the tracking of photoelectrons with subas precision,[41] the direct observation of electron propagation and dielectric screening on the atomic scale,[42] attosecond nanoscale near-field sampling,[43] and electron localization in the dissociative ionization of H_2 and D_2.[44] Attosecond pump–probe spectroscopy has also been realized in condensed matter,[45] for example, the observation of optical field-induced current in dielectrics,[46] the control of dielectrics with the electric field (e-field) of light,[47] and the direct observation of electron propagation and dielectric screening on the atomic scale.[48] Additionally, the attosecond transient absorption technique, which involves measuring the changes in the XUV spectrum transmitted through the sample induced by the NIR pulses, was developed to study the relevant ultrafast dynamics in the sample.[36–38] With attosecond transient absorption spectroscopy, an experimental study elucidating the impact of electronic correlations on the electron dynamics was performed for the first time,[49] and the time-resolved autoionization of Ar[50] and real-time observation of valence electron motion were demonstrated.[51]

Until now, attosecond streaking spectroscopy and transient absorption spectroscopy have given rise to remarkable achievements in both the characterization of attosecond pulses and the pump–probe experiments.

However, these two methods only provide energy-resolved measurement, while many applications require angular-, momentum-, spatial-, and/or spin-resolved measurements for studies on the electronic structure of superconductors, magnetic materials, nano-plasmonic structures, surfaces, atoms, molecules, etc. Angle-resolved photoelectron spectroscopy (ARPES),[52,53] photoemission electron microscopy (PEEM),[54,55] and cold-target recoil-ion momentum spectroscopy (COLTRIMS)[56,57] are typical photoemission spectroscopy (PES) methods with widespread practical applications in many fields for elucidating the electronic structures in solid-state physics, chemistry, and biology. In previous studies, the light sources for PES were a traditional mercury lamp, a noble-gas discharging lamp, and synchrotron radiation.[58] With the advent of HHG and single attosecond pulses, table-top XUV light sources have become ideal drivers for time-resolved PES because these types of coherent radiation have good spatial profiles, broadband tunable spectra covering ultraviolet (UV) to soft x-ray, and high flux with durations ranging from tens of attoseconds to tens of femtoseconds.

The first time-resolved ARPES (tr-ARPES) using an HHG source was developed by the Department of Physics at the University of Kaiserslautern in Germany.[59] The HHG light source was driven by a Ti:sapphire laser at a repetition rate of 1 kHz. A pair of XUV multilayer mirrors were used to select XUV light at 41.85 eV, and a combination of IR and XUV beams was focused onto the target in the ARPES chamber to perform time- and angle-resolved PES. Because no monochromator was installed to select a narrow band of HHG and a low repetition rate, the energy resolution of the tr-ARPES was approximately 1 eV, which was too low to obtain any electronic structures of the Fermi band in solids. The aforementioned HHG system was then updated to use the second harmonic of a Ti:sapphire laser at a higher repetition rate (10 kHz) in 2014.[60] The larger separation of the harmonic orders driven by the second harmonic allowed the omission of all dispersive elements and the monochromator in the HHG beam, and intrinsic narrow-bandwidth harmonics were obtained. Finally, the energy resolution was improved to 150 meV, and a temporal resolution of approximately 30 fs was also demonstrated. Snapshots of the photoinduced electronic-structure changes of $TiSe_2$ were obtained using the updated tr-ARPES. In 2006, the Rutherford Appleton Laboratory started to build a comprehensive facility (Artemis) that offers ultrafast XUV (10–100 eV) pulses produced through HHG.[61] The vacuum beamlines deliver synchronized pulses to end-stations, which have three application apparatuses for condensed-matter physics, atomic and molecular physics, and XUV imaging. A key application at Artemis is time- and angle-resolved photoelectron spectroscopy using tr-ARPES. To improve the energy resolution, an XUV monochromator was designed to cover two spectral ranges (12–30 nm and 30–90 nm) with either a higher resolving power or a shorter pulse duration. The energy resolution was demonstrated to be 130 meV.[62] Thus far, tr-ARPES has been successfully applied for both time- and angle-resolved photoemission measurements on numerous materials, including graphene and topological insulators, such as the time-resolved photoemission measurement of TaS_2 at a low temperature,[63] snapshots of the non-equilibrium Dirac carrier distributions in graphene,[64] the ultrafast dynamics of massive Dirac fermions in bilayer graphene,[65] and tunable carrier multiplication and cooling in graphene.[66] Additionally, earlier this year, the dynamics of correlation-frozen antinodal quasiparticles in superconducting cuprates were examined via tr-ARPES.[67] The limitations of the tr-ARPES at Artemis are the low repetition rate (1 kHz) and the space-charge effect in the interac-

tion area; thus, the laser system is currently being upgraded to a 100 kHz OPCPA system operating at 1.7 μm. Worldwide, many other tr-ARPES systems have been developed. A tr-ARPES system at Freie Universität in Berlin[68] with an energy resolution of 90 meV and a temporal resolution of 125 fs was constructed. Studies on the disparate ultrafast dynamics of itinerant and localized magnetic moments in Gd metal were performed.[69] Keller group in Switzerland developed a versatile attosecond beamline for time-resolved measurements, in which a tr-ARPES system was included.[70] A similar facility was developed at Max-Planck-Institut für Quantenoptik in Germany.[71] Los Alamos National Laboratory reported a tr-ARPES system in which a time-delay compensated monochromator was used to preserve the ultrashort duration of the XUV pulses in a wide tunable range of photon energies (20–36 eV) at a repetition rate of 10 kHz, and the capabilities to obtain angle-resolved photoemission maps and to trace ultrafast the electron dynamics in an optically excited semiconductor were demonstrated.[72] The HELIOS laboratory at Uppsala University in Sweden designed a pump–probe XUV source for ARPES called Scienta ARTOF 10k (ARTOF: angle-resolved time of flight). After successful tests, it was upgraded to ARTOF 2.[73] The CITIUS facility is a state-of-the-art HHG light source at the University of Nova Gorica in Slovenia, where an innovative monochromator allows researchers to work in time-preserving or high-resolution regimes; here, ARTOF was used for pump–probe experiments.[74]

Currently, a well-developed ARPES system can achieve a very high energy resolution of approximately 1 meV. However, a tr-ARPES system cannot achieve high energy and high temporal resolution simultaneously. The high energy resolution of an ARPES system requires a very narrowband light source, which corresponds to a long pulse duration. As a tradeoff between the energy and temporal resolutions, the combination of approximately 100 fs and approximately 30–50 meV is a good choice for most experiments in condensed matter. It is also important to avoid degradation of the resolution caused by the space-charge effect of the photoelectrons. It is necessary to reduce the XUV intensity to a level where one electron or fewer is generated per laser shot. To achieve such a low count rate but keep the data acquisition reasonably short, it is necessary to increase the repetition rate of the driving laser while reducing the energy of each laser pulse to eliminate the space-charge effect so that an adequate average photon and thus the photoelectron flux is maintained. Therefore, the driving femtosecond laser for the ARPES is chosen to have a repetition rate of at least 100 kHz. In contrast to the hemispherical electron analyzer, ARTOF can measure a large part of the K-space without moving the sample and can operate at a low XUV intensity to reduce the space-charge effect because of its large collection angle. The development of time-resolved ARTOF using low-intensity XUV pulses at a high repetition rate is important for the angle- and time-resolved measurement of photoelectrons.

A traditional attosecond streak camera maps the e-field and thus the time of the NIR pulse to the momentum or energy distribution of the photoelectrons, whereas in attosecond angular-streaking spectroscopy, which is also called "attoclock," time is mapped to the angular distribution of the photoelectrons. The momentum distribution of the photoelectrons is obtained using elliptically polarized laser pulses in which the e-field vector rotates in the polarization plane. It illustrates the emission angle of the photoelectrons and the direction of the e-field vector at the time of emission, thus providing timing information regarding the laser e-field oscillation. The e-field vector runs 360° in one optical cycle of 2.7 fs at a central wavelength of 800 nm, and it is relatively easy to accurately measure the momentum distribution of the photoelectrons; thus, the precision for determining the timing in this kind of experiment can be well below one optical period. COLTRIMS can measure the three-dimensional (3D) momentum vectors of the fragments (electrons and ions) originating from one ionization or dissociation event coincidently. Attosecond angular streaking was first realized with a combination of CEP-controlled near-circularly polarized 5-fs laser pulses and COLTRIMS by Keller group.[75] Attoclock measurement can provide a temporal resolution of 200 as and a direct measurement of the CEP with an accuracy of 60 mrad. By using the attoclock technique, numerous attosecond timing measurements have been performed, including the ionization and tunneling delay time in He,[76] the tunnel geometry,[77] and the timing of sequential double ionization.[78,79] Many other groups have constructed ultrafast COLTRIMS using typical femtosecond laser pulses having durations ranging from a few femtoseconds to tens of femtoseconds with CEP-stabilization, and progress has been achieved.[80–83] With the advent of HHG and related techniques, XUV pulses with tunable high-energy photons and pulse durations as short as sub-femtosecond have introduced the possibility of accessing the inner-shell and inner-valence ionization of highly excited atoms and molecules in the gas phase; thus, the combination of HHG XUV sources and COLTRIMS yields the most powerful tool for studying the photofragmentation dynamics of highly excited states in atoms, small molecules, or surface reactions with sub-femtosecond resolution. The pioneering XUV-COLTRIMS was constructed using an HHG source driven by a Ti:sapphire laser at repetition rates varying between 1 kHz and 3 kHz,[84] and the dissociation of a molecule ionized by soft x-ray radiation was observed in real time.[85] Another early XUV beamline combined with reaction microscopy for investigation of the attosecond dynamics of atoms and molecules was developed at Max-Planck-Institut für Kernphysik, using a Ti:sapphire laser with a repetition rate ranging from 3 kHz to 10 kHz.[86] Later, the XUV source was upgraded using CEP-stabilized few-cycle laser

pulses. Other prototype XUV-COLTRIMS beamlines were developed at JRM Lab of Kansas State University[87–89] and at Laser Interactions and Dynamics Laboratory in France.[90] All the aforementioned XUV-COLTRIMS beamlines are based on HHG attosecond pulse trains (APTs). The first combination of single XUV attosecond pulses with a COLTRIMS apparatus, which was called AttoCOLTRIMS, was successfully developed by Keller *et al.*[91] The attosecond beamline was constructed using 5-fs CEP-stabilized laser pulses at a repetition rate of 10 kHz, the single attosecond pulse was generated using the PG method, and the duration of the XUV pulses was characterized to be 280 as at 45 eV using a 3D streaking spectrogram based on AttoCOLTRIMS. As milestone experiments using AttoCOLTRIMS, the relative photoemission delays were successfully measured even though the photoelectrons from a mixture of Ar/Ne overlapped in the spectrum,[92] and the resonance effects in the photoemission time delays were characterized.[93]

PEEM is an advanced surface analysis technique that has been under development since the 1990 s and is capable of imaging the surface electronic structure by recording photoelectrons emitted from the surface of a sample in response to the absorption of ionizing radiation such as UV or x-ray photons. The electrons are collected, and the image is magnified hundreds- or thousands-fold through a series of magnetic or electrostatic electron lenses. Because PEEM constructs images from photoelectrons emitted from the entire surface directly without two-dimensional (2D) scanning as in a scanning tunneling microscope, it is suitable for studying surface dynamics, especially for imaging complex layered thin films or devices in real time. As a brand new surface analysis technique, PEEM has very important applications in research areas such as thin-film growth, surface chemistry, surface magnetism, and surface electronic states to study surface electronic structures via *in situ* and real-time imaging. With the development of surface science and time-resolved measurement technology, researchers wish to discover not only the distribution of surface electrons but also the change of the characteristics over time, giving rise to time-resolved PEEM (tr-PEEM). In the early stage, PEEM was successfully developed for imaging of plasmonic fields with femtosecond temporal resolution using two-photon photoemission (2PPE) based on a Ti:sapphire femtosecond oscillator.[94] With the advent of HHG and related techniques, utilizing a pair of attosecond and femtosecond pulses for pump–probe spectroscopy, Stockman proposed attosecond nanoscope or atto-PEEM, which is a combination of PEEM with attosecond streaking technology for non-invasive and direct access of nanoplasmonic fields with nanometer (spatial) and attosecond (temporal) resolutions.[95] Soon thereafter, atto-PEEM was developed at Lund University, Ludwig Maximilian University of Munich, and Max-Planck-Institut für Quantenoptik. L'Huillier group in Lund University developed an attosecond-resolved PEEM system using APTs[96] at a repetition rate of 1 kHz, and a spatial resolution of 300 nm was demonstrated.[97] The Kleineberg group in Ludwig Maximilian University of Munich and Max-Planck-Institut für Quantenoptik constructed an atto-PEEM system using single attosecond XUV pulses[98] based on an existing attosecond beamline. The first PEEM experiment involving excitation by single attosecond XUV pulses was reported in 2012,[99] driven by CEP-controlled 5-fs laser pulses at a repetition rate of 1 kHz, and a spatial resolution of 300 nm and a temporal resolution of 350 as were simultaneously demonstrated. In these two proof-of-principle experiments using APTs and single attosecond pulses, the spatial resolution was hundreds of nanometers and was limited by the aberrations of the electron optics in PEEM and the space-charge effect in the interaction area. Clearly, this limitation can be reduced by increasing the repetition rate of the driving laser. A high-repetition rate system can reduce the exposure time and space charge by more than an order of magnitude. Thus, attosecond pulses with repetition rates over hundreds of kilohertz are crucial for the improvement of the spatial resolution in Atto-PEEM. Many groups are currently developing new attosecond sources at higher repetition rates. L'Huillier group is developing an OPCPA laser with a high repetition rate (200 kHz–2 MHz) for generating XUV pulse trains,[100] and Kleineberg group developed a new attosecond source with a high repetition rate of 10 kHz.[101]

Considering the advancements of XUV beamlines based on HHG and the many aforementioned applications, the main objective of the attosecond laser station (ALS) at the Synergetic Extreme Condition User Facility (SECUF) in Huairou, Beijing is to develop XUV beamlines for investigating the electron dynamics in atoms, molecules, and condensed matter on timescales ranging from tens of femtoseconds to hundreds of attoseconds. The ALS has four XUV beamlines for different end-stations that aim to study the ultrafast dynamics in atoms and molecules, condensed matter, surfaces, and nano-plasmonic structures, which are similar to Extreme Light Infrastructure (ELI) Attosecond Light Pulse Source (ELI-ALPS).[102] The first beamline is a high energy sub-100-as XUV beamline with a center photon energy of approximately 90 eV, which is driven by high-energy sub-10-fs laser pulses at a repetition rate of 1 kHz. The beamline is designed to combine with an attosecond streaking camera and an XUV spectrometer to perform attosecond streaking spectroscopy and transient absorption spectroscopy for characterizations of the electron dynamics in atomic and molecular gases, condensed matter, and surfaces. The second beamline has a high repetition rate and a narrowband XUV spectrum, driven by a high-power femtosecond fiber laser at repetition rates of 200 kHz to 1 MHz. The beamline is designed to integrate a monochromator and an ARPES system as an end-station to realize angle-

and time-resolved photoelectron spectroscopy for studying the dynamics of excitons in solid-state structures and investigating the band structures near the Fermi level in strongly correlated materials in real time to obtain an in-depth understanding of the superconductivity. The third beamline is a single attosecond broadband XUV beamline driven by CEP-stabilized sub-10-fs Ti:sapphire laser pulses at a repetition rate of 10 kHz. This beamline is designed to employ attosecond pulses with COLTRIMS for attosecond transient photoelectron–photoion spectroscopy coupled with coincidence measurement pump–probe spectroscopy to investigate laser-induced molecular dissociative ionization by measuring 3D momentum vectors of all dissociation fragments. The fourth beamline can produce broadband XUV attosecond pulses with a higher repetition rate, driven by CEP-stabilized sub-10-fs OPCPA laser pulses at a repetition rate of 100 kHz. This beamline is designed to employ single attosecond XUV pulses with PEEM to realize transient measurements of the plasmonic structure and nanostructure with high temporal and spatial resolutions.

2. Design of ALS

The XUV radiation based on HHG has unique properties of spatial and temporal coherence with tunable central photoenergy ranging from 10 eV to hundreds of eV and pulse duration ranging from tens of attoseconds to tens of femtoseconds and is an ideal light source for probing and controlling ultrafast phenomena such as electron dynamics. In the ALS, the four XUV beamlines are designed to integrate different end-stations with corresponding XUV sources for momentum-resolved and spatially resolved (simultaneously or independently) measurements of ultrafast dynamics in atoms, molecules, and condensed matter on timescales ranging from tens of femtoseconds to hundreds of attoseconds and form a comprehensive experimental platform to investigate electron dynamics by such ultrafast XUV coherent radiation coordinated with precisely tailored femtosecond laser fields, as shown in Fig. 1.

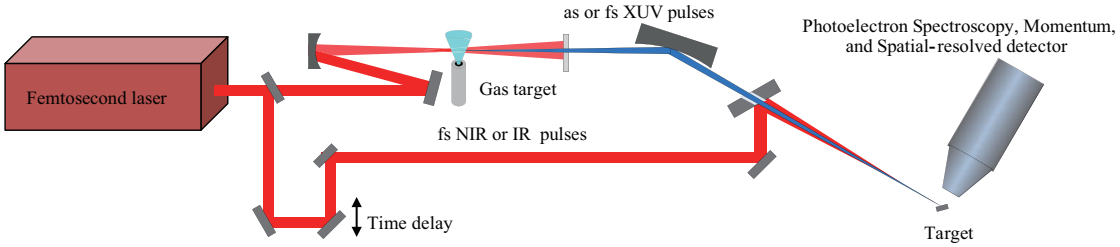

Fig. 1. (color online) Principle of attosecond pump–probe spectroscopy.

The concept of the attosecond pump–probe scheme is as follows. One femtosecond laser pulse is split into two with a variable time delay. The first laser pulse is focused into a noble gas to generate an XUV pulse, which, after spectral selection and/or temporal stretching/compressing, is focused onto a gas or solid target to excite or ionize an electron or initiate a charge migration process in the cation of the target. After a well-controlled amount of time, a second laser pulse further excites or ionizes the target or modulates the momentum of the already ionized photoelectron with a precisely tailored short NIR or IR laser field. The measurements are repeated for a series of time delays between the two pulses. A stroboscopic movie of electronic movement or charge-transfer processes is then obtained to study the ultrafast dynamics in atomic, molecular, and condensed-matter systems.

The four beamlines in the ALS serve four complex apparatuses: (i) electron time-of-flight (e-TOF) with a high energy resolution and a flat-field XUV spectrometer for attosecond streaking and transient absorption measurements to characterize single attosecond pulses and investigate attosecond resolved dynamics of electrons in atoms, molecules, and condensed matter; (ii) ARPES for attosecond time-resolved photoelectron spectroscopy (tr-ARPES) utilizing the high momentum and energy resolutions of ARPES to measure the dynamics of excitons in solid-state structures and investigate band structures near the Fermi level in strongly correlated materials in real time to obtain an in-depth understanding of the superconductivity; (iii) COLTRIMS for attosecond transient photoelectron–photoion spectroscopy with capabilities of coincident measurement and pump–probe spectroscopy to investigate laser-induced molecular dissociative ionization by measuring 3D momentum vectors of all dissociation fragments; and (iv) PEEM for attosecond transient surface photoelectron spectroscopy, combining the high temporal resolution of the XUV radiation with the high spatial resolution of PEEM to study the ultrafast electron dynamics on the surface or in nanostructures.

Considering current state-of-the-art applications of attosecond XUV radiation and future development of attosecond science, four attosecond and femtosecond light sources in the XUV range are developed to drive the experimental end-stations described previously, including two beamlines for atomic, molecular, and optical physics (attosecond streak camera and COLTRIMS) and two beamlines for condensed-matter physics and material science (PEEM and ARPES), as shown in Fig. 2.

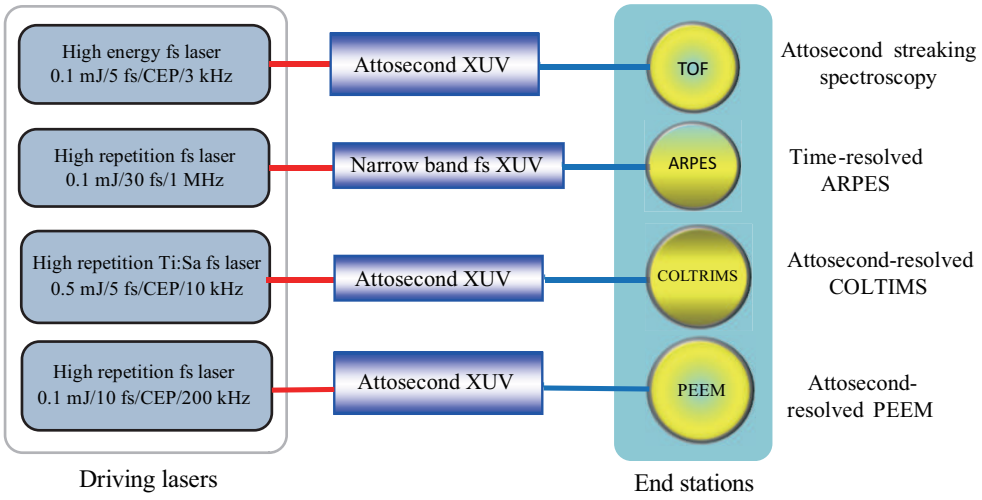

Fig. 2. (color online) Layout of the ALS.

The driving laser for the attosecond streak camera (AttoSC) beamline is a CEP-locked sub-10-fs laser with a repetition rate of 1 kHz and a pulse energy of 3 mJ. The generated broadband single attosecond XUV pulse is collimated, recombined with a part of the femtosecond pulse, and focused together onto the second target to produce photoelectrons that enter the time-of-flight (TOF) of the attosecond streak camera. At the same time, the XUV spectrum transmitted through the target is measured by an XUV spectrometer to obtain transient absorption spectra. The femtosecond driving laser for the ARPES beamline has a repetition rate of 1 MHz. A monochromator is employed to pick an appropriate narrow band ($<$ 100 meV bandwidth) from the XUV radiation, which is then focused by a toroidal mirror into the ARPES analyzer to perform time- and angle-resolved PES. The driver of the COLTRIMS beamline is a CEP-locked sub-10-fs laser with a repetition rate of 10 kHz and a pulse energy of 1 mJ. The generated broadband single attosecond pulse is recombined with a small part of the driving laser pulse and enters the COLTRIMS detector for atto-COLTRIMS experiments to study transient atomic and molecular structures and electron correlation mechanism with attosecond temporal resolution. In the PEEM beamline, the attosecond XUV pulses driven by a CEP-locked sub-10-fs laser with a 100-kHz repetition rate are focused by a toroidal mirror into the PEEM detector to conduct atto-PEEM measurements to investigate ultrafast phenomena on atomic scales with unprecedented temporal and spatial resolutions. The four beamline in the ALS will have fluxes of 10^9 to 10^{12} photon/s in a tunable range of 20 eV to 100 eV for versatile end stations. Table 2 compares the specifications of the ALS with those of other HHG beamlines, seeded FELs, and SASE FELs.

Table 2. Comparison of ALS (SECUF) and other XUV light sources based on HHG, seeded FEL, and SASE FEL.

	Generation	Duration	Flux/(photons/s)	Tuning range/eV	Rep. rate	Peak power/GW	Ref.
ELI-ALPS	HHG	$<$ 100 as	1.25×10^{12}	10–120	1–100 kHz	10^{-3}	[102]
ALS (SECUF)	HHG	$<$ 100 as to 200 fs	10^9–10^{12}@20–30 eV	20–100	1 kHz to 1 MHz	10^{-3}	this paper
Artemis (RAL)	HHG	10–50 fs (APT)	1.8×10^9@30 eV	10–100	1 kHz	unspecified	[103]
LCLS (SLAC)	SASE FEL	10–1000 fs	10^{14}	500–800	120 Hz	$\sim$ 60	[104]
Dreamline (SSRF)	SASE FEL	unspecified	3.5×10^{11}@800 eV	20–2000	2 Hz	unspecified	[105]
FLASH (DESY)	SASE FEL	50–200 fs	10^{12}–10^{14}	24–310	10 Hz	$\sim$ 2.5	[106], [107]
FERMI (Elettra ST)	seeded FEL	150 fs	3.7×10^{13}	15.5–62	10 Hz	0.2	[108]
DCLS (Dalian)	seeded FEL	30/130/1000 fs	$> 2.5 \times 10^{13}$	8.3–25	unspecified	0.1	[109]

The details of the design for each beamline are presented as follows.

2.1. Beamline for attosecond streaking and transient absorption spectroscopy (AttoSC)

The beamline is designed to generate IAPs at approximately 90 eV, which are collinearly collimated with the NIR beam and focused onto a second target (gas or solid) to perform attosecond streaking experiments, and the transmitted XUV light is detected by an XUV spectrometer to perform attosecond transient absorption experiments. The characterization of a single attosecond pulse can be realized in the beamline, and the measurements of the electron dynamics in atomic, molecular, and condensed matter systems can be performed using an attosecond streak camera and/or a transient absorption spectrometer.

The beamline is composed of the driving laser, the HHG chamber, the filter and toroidal mirror chamber, the e-TOF chamber, and the XUV flat-field spectrometer. The layout of the beamline is shown in Fig. 3.

The driving laser for the single attosecond beamline is a CEP-stabilized sub-10-fs laser with a pulse energy of 3 mJ, which is produced by spectral broadening in a hollow fiber and compression with chirped mirrors. The CEP of the laser system is controlled by two separated feedback loops, one of which is a fast loop to stabilize the laser pulses from the oscillator and the other is for stabilization of the amplified pulses by controlling the displacement of one prism in the compressor according to the feedback signal from an f–$2f$ spectral interferometer installed after the hollow fiber. The singleshot CEP fluctuation is < 300 mrad. XUV HHG radiation is generated by focusing the driving laser pulses into a quasi-static gas cell, and IAPs are produced via the AG scheme. The continuous spectrum in the HHG cutoff region is selected by a metallic filter to obtain a single attosecond pulse, which is recombined with a small part of the NIR pulse and focused onto the second target (gas or solid). The attosecond XUV pulses first ionize the second target to produce photoelectrons, and then the photoelectrons are shifted in the momentum space by an amount that depends on the vector potential of the NIR field at the time when the XUV and IR pulses overlap in space and time. To stabilize the time delay between the XUV and IR pulses, an active interferometer stabilization scheme is adopted. A single-mode green laser is used to pass through all the same optical components of both pump and probe arms in the XUV–IR pump–probe configuration, which is a Mach–Zehnder interferometer, to produce interference patterns in real time. By sending a feedback signal derived from the interference pattern to a piezo translation stage in the pump beam to control the time delay between the XUV and IR pulses, long term stability with sub-100-as (RMS) is realized. With the active interferometer stabilization, by scanning the time delay between the XUV and IR pulses, the modulated photoelectron energy spectra at a series of delays form an attosecond streaking spectrogram. Characterization of the single attosecond pulse and transient measurements of the electronic dynamics in matter can be achieved via the attosecond steaking trace. Regarding the transmitted XUV pulses, a spectrometer is employed to obtain absorption spectra at different delays between the XUV and IR pulses, which compose a transient absorption spectrogram.

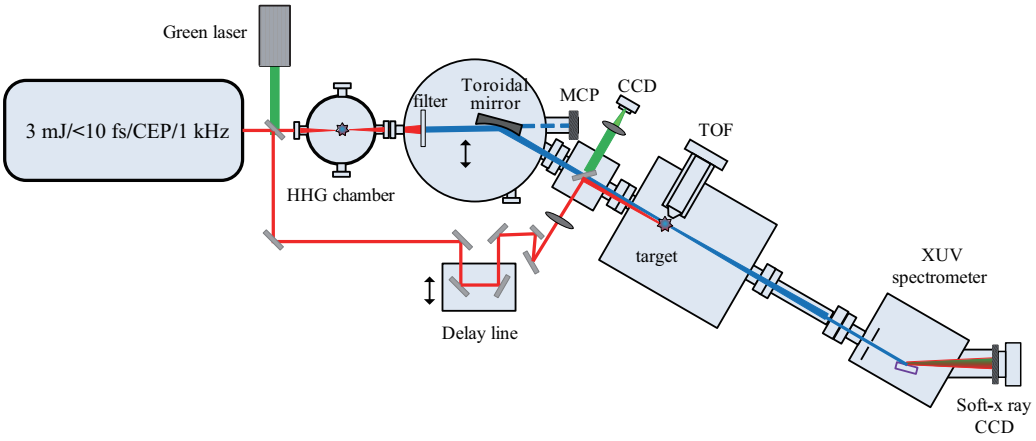

Fig. 3. (color online) Beamline for single attosecond pulse generation, attosecond streaking spectroscopy, and transient absorption spectroscopy.

The beamline will have pulse durations of < 100 as at the XUV spectral range of 30 eV to 100 eV. It can facilitate research on attosecond streaking spectroscopy and transient absorption spectroscopy.

2.2. Beamline for attosecond time-resolved photoelectron spectroscopy with ARPES

ARPES is the most intuitive tool for studying material band structures and is potentially the most powerful device for exploring crucial physical phenomena in high-T_c superconductivity studies. Via momentum and energy measurements of the photoelectrons with ultrahigh resolutions, the kinetic energy and momentum of the excitons inside the materials may be obtained. Extending ARPES to the ultrafast timescale makes it possible to observe the electron dynamics in real time and to distinguish various excitations on different timescales, providing a new route to study quantum materials. Tr-ARPES is capable of collecting multidimensional data regarding the energy, momentum, and time of the electron dynamics in different momentum spaces by capturing movies of the electron energy spectra during phase transitions, thus revealing the formation of superconducting Cooper pairs. This type of data may reveal key features of the insulator–superconductor phase transition and provide direct experimental evidences for the high-T_c superconducting mechanism.

Tr-ARPES is a new type of measurement combining the

temporal resolution of a pump–probe configuration and the energy and momentum resolutions of ARPES. To avoid degradation of the energy resolution caused by the space-charge effect of the photoelectrons, it is necessary to reduce the photon number in each XUV pulse and to increase the repetition rate simultaneously to maintain an adequate average flux of the photoelectrons for experimental data acquisition. The repetition rate must be at least 100 kHz for the driving femtosecond laser. A schematic of the beamline for tr-ARPES based on HHG is shown in Fig. 4.

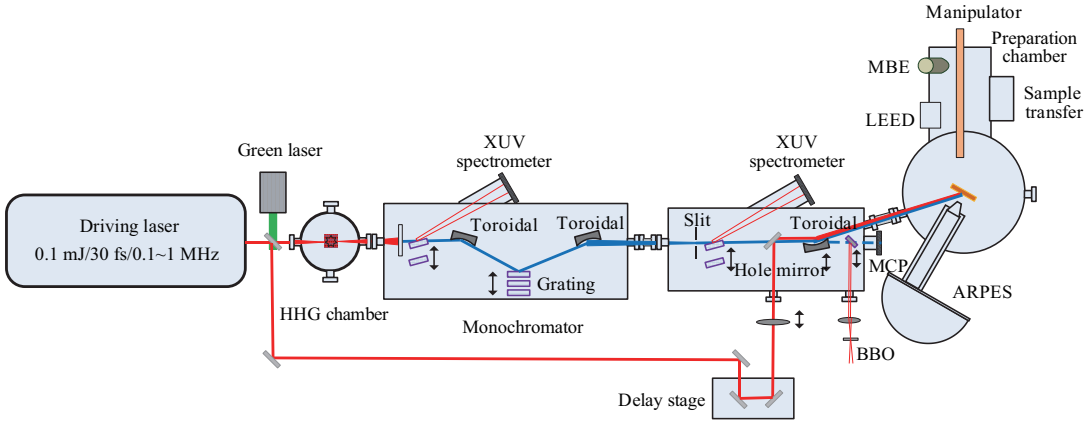

Fig. 4. (color online) Schematic of the beamline for tr-ARPES.

The beamline for tr-ARPES comprises a high-repetition rate femtosecond laser, an HHG chamber, a monochromator, an XUV spectrometer, a toroidal focusing chamber, and an ARPES analyzer.

As described previously, narrowband XUV pulses at a very high repetition rate are crucial for tr-ARPES; therefore, a high-power femtosecond fiber laser is employed, which has a pulse energy of 0.5 mJ with 40-fs pulse duration at a repetition rate of 1 MHz, but CEP stabilization is not necessary. The laser pulses are focused onto an Ar target in the HHG chamber to generate XUV pulses that have energies ranging from 20 eV to 50 eV. A monochromator is designed to obtain a very narrow band from the HHG. The monochromator has two toroidal mirrors, two grating groups, and two slits. The HHG beam is collimated by the first toroidal mirror and deflected onto the grating. The diffracted HHG is then refocused by the second toroidal mirror onto the slit to obtain narrowband XUV light. The selected narrowband HHG is relay-imaged by another toroidal mirror onto the target in the ARPES analyzer. The pump beam is split from the main laser or a synchronized IR optical parametric amplification (OPA), recombined with the XUV beam through a delay line, and collinearly focused onto the same target to measure the photoelectron dynamics. An active interferometer stabilization scheme using a single-mode green laser is also implemented for long term stabilization between the pump and probe pulses in the beamline.

The monochromator is the key component in the tr-ARPES beamline. It is used to obtain a very narrowband XUV spectrum from a single harmonic in HHG. The monochromator design is based on a single-grating diffraction scheme, but gratings with different groove densities will realize different spectral resolutions. Considering that both a high energy resolution and a high temporal resolution must be realized by the monochromator, two groups of gratings with a double-switching configuration are employed.[110,111] One grating group is aligned in the classic diffraction geometry for obtaining a high spectral resolution but with longer XUV pulse durations, and the other group is aligned in the off-plane geometry for preserving shorter pulse durations but with low spectral resolution. The minimum spectral resolution of the classic geometry is calculated to be < 60 meV, while the temporal resolution is < 200 fs when the grating groove densities of 150 mm^{-1}, 300 mm^{-1}, and 600 mm^{-1} are adopted for the energy range of 20–60 eV. For the off-plane geometry, the temporal resolution will be < 100 fs and the energy resolution will be > 100 meV when the grating groove densities of 500 mm^{-1}, 900 mm^{-1}, and 1800 mm^{-1} are adopted for the same energy range. The double configurations of the grating mounts can be switched by a motorized translation stage according to the experimental requirement of a high energy resolution or an ultrafast response.

The specifications of the ARPES analyzer are that the energy resolution is < 3 meV at 20–30 eV, the angular resolution is $< 0.1^\circ$, and the sample temperature can be as low as ~ 4.2 K. When this XUV beamline is integrated with the ARPES analyzer, tr-ARPES can provide a temporal resolution of < 200 fs and an energy resolution of < 60 meV in the range of 20–50 eV simultaneously for measurements of band structures in solid-state materials.

2.3. Beamline for attosecond transient photoelectron–photoion spectroscopy with COLTRIMS

Combining a supersonic cold target, charged particle detectors, and 3D momentum measurement techniques,

the COLTRIMS is capable of completely and coincidently quantifying the kinematics of ions and electrons to obtain 3D momentum imaging of all final fragments of each laser–atom/molecule interaction event. Key components of COLTRIMS include (i) an ultra-high vacuum (UHV) target chamber, (ii) a supersonic atomic or molecular beam, (iii) TOF systems, (iv) 2D position-sensitive detectors, (v) front-end electronics, and (vi) a data-acquisition system. The ultrahigh-density gas target from the supersonic atomic or molecular beam interacts with intense laser pulses. The end product of the interaction, including ions and electrons, travels through the corresponding TOF system to be captured by the corresponding position-sensitive detector. The geometric and quantum configurations of atoms or molecules at the time when the ionization, dissociation, or collision occurs can be derived from the positions and TOFs of the charged particles detected in coincidence. By using the acquired data, the fragmentation dynamics of atoms and molecules initiated by ultrashort laser pulses can be fully analyzed. In the beamline, the combination of single attosecond XUV pulses with COLTRIMS is developed to investigate the ultrafast dynamics of electrons and nuclei in highly excited molecular ions with sub-femtosecond temporal and high momentum resolutions.

The schematic of the beamline for COTRIMS is shown in Fig. 5. The beamline comprises a driving laser system with CEP-controlled 5-fs pulses at 10 kHz, an HHG chamber, transport and focusing chambers of the XUV beam, a COLTRIMS system, and an XUV spectrometer.

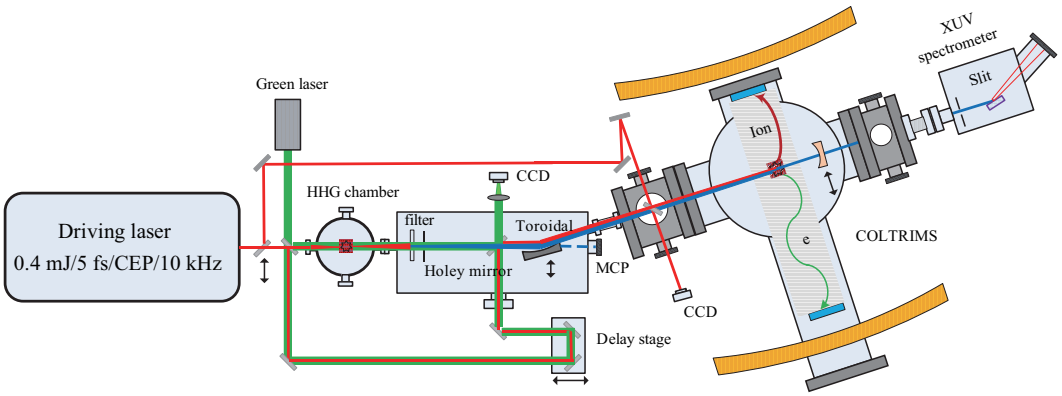

Fig. 5. (color online) Attosecond transient photoelectron–photoion spectroscopy with COLTRIMS.

A CEP-locked 1-mJ sub-5-fs laser operating at a 10-kHz repetition rate is employed to drive single attosecond XUV pulse generation. The sub-5-fs laser pulses will be obtained via spectral broadening and compression by chirped mirrors, and the CEP stabilization will be realized by two controlling loops using f–$2f$ spectral interferometry techniques. The laser pulse is focused onto a noble-gas target to drive HHG. Using AG, the continuous spectrum in the HHG cutoff region can be selected using a metallic filter, which corresponds to an IAP. The XUV pulse is recombined with a small part of the driving laser split from the main beam and focused by a toroidal mirror onto the supersonic cold target in the COTRIMS system to perform XUV–IR pump–probe experiments. An XUV spectrometer is located behind the COTRIMS system to obtain the spectrum of the XUV pulses. A single-mode green laser is used to implement the active interferometer stabilization scheme to realize long-term stability between the pump and probe pulses with sub-100-as (RMS). With the actively stabilized interferometer, the beamline will have the following specifications: a temporal resolution less than 200 as and a momentum resolution (COLTRIMS) of < 0.1 a.u. (atomic unit) for ions and 0.05 a.u. for electrons. Moreover, it will allow users to analyze time-resolved 3D momenta of all the fragments from laser–atom or laser–molecule reactions.

2.4. Beamline for attosecond transient surface photoelectron spectroscopy with PEEM

PEEM can provide highly spatially resolved measurement; thus, it has important applications in research areas such as thin-film growth, nano-plasmons, surface chemistry, surface magnetism, and surface electronic structures via *in situ* and real-time imaging. With the development of surface science and time-resolved measurement technology, researchers wish to discover not only the distribution of surface electrons but also the change of the characteristics in time, giving rise to tr-PEEM. The main idea of the beamline is to generate an isolated attosecond XUV pulse for the PEEM to realize high spatial and temporal resolutions in measurements. A schematic of the beamline for attosecond time-resolved PEEM is shown in Fig. 6.

The beamline comprises a CEP-locked femtosecond laser with a pulse energy of 0.1 mJ at a repetition rate of 100 kHz, an HHG chamber, a toroidal mirror chamber, a PEEM analyzer, and an XUV spectrometer.

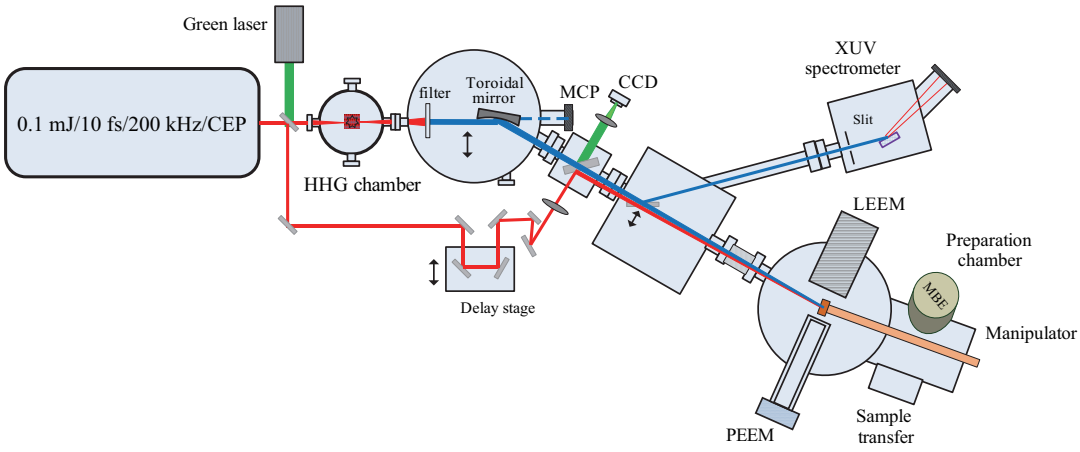

Fig. 6. (color online) Beamline for attosecond time-resolved PEEM.

To eliminate the space-charge effect in the interaction area and improve the spatial resolution of PEEM, as described in the introduction section, a laser operating at a repetition rate of $>$ 100 kHz that delivers CEP-controlled sub-10-fs pulses with energy of 0.1 mJ is employed to generate single attosecond pulses. The laser is developed according to the optical parametric chirped-pulse amplification (OPCPA) technique, whose seed is a passively CEP-stabilized pulse obtained from differential frequency generation of the supercontinuum. The seed pulse is amplified in three non-collinear OPA stages pumped by high-power picosecond 515-nm laser pulses. The amplified laser pulse has energy of 0.15 mJ with a spectral range of 700–1000 nm and is compressed to sub-10-fs by chirped mirrors. After the compression, an f–$2f$ interferometer is employed to further stabilize the CEP, and the fluctuation of the CEP will be $<$ 210 mrad for single-shot measurements.

The few-cycle OPCPA laser is focused onto a noble gas target by an off-axis parabolic mirror in the HHG chamber to generate an IAP using AG. The attosecond pulse passing through a metal filer is selected and recombined with the pump beam, which is derived from the main beam or the IR OPA at a central wavelength ranging from 1.1 μm to 2.6 μm. The attosecond beam and the pump beam are collinearly focused onto the target in PEEM to form the pump–probe configuration and realize attosecond time-resolved and nanometer spatially resolved measurements. An active interferometer stabilization scheme between the pump and probe beams using the aforementioned single-mode green laser is employed to ensure long-term stabilization of the pump–probe pulses. A Si plate installed on a motorized translation stage is used to reflect XUV pulses to a spectrometer to obtain the XUV spectrum. A TOF-PEEM is used to detect the photoelectrons with special energy selective filtering; thus, the electron optical aberration will be reduced, and the spatial resolution will be improved. Attosecond streaking spectroscopy can also be realized using this TOF-PEEM to characterize the attosecond pulses.

The beamline using high-repetition rate few-cycle laser pulses is designed for PEEM, which allows measurements with a spatial resolution of $<$ 30 nm and a temporal resolution of 200 as to study the ultrafast dynamics of nano-plamonic structures and surfaces.

To supplement the aforementioned design details, the specifications for the four beamlines in the ALS are summarized in Table 3.

Table 3. Specifications of the beamlines in ALS-SECUF.

	Rep. rate	Spectral range	Duration	Flux /(photon·s^{-1})	Energy/momentum resolution	Spatial resolution	End station
Beamline 1	1–3 kHz	30–100 eV	$<$ 100 as	$\sim 10^9$–10^{10}	$<$ 0.5 eV	unspecified	e-TOF/XUV spectrometer
Beamline 2	1 MHz	20–80 eV, tunable	$<$ 200 fs	10^{11}	$<$ 50 meV	unspecified	ARPES
Beamline 3	10 kHz	50–100 eV	$<$ 200 as	10^{10}	$<$ 0.1 a.u. (ion) $<$ 0.05 a.u. (electron)	$<$ 100 μm	COLTRIMS
Beamline 4	100 kHz	60–96 eV	$<$ 200 as	10^{11}	$<$ 80 meV	$<$ 30 nm	PEEM

3. Research progress

Supported by the National Natural Science Foundation of China (NSFC), Ministry of Science and Technology (MOST) of China, and the Chinese Academy of Sciences, our team has been involved in research on the generation, characterization, and applications of attosecond pulses since 2003. Because a few-cycle laser pulse with CEP stabilization is crucial for the generation of isolated attosecond XUV pulses, our research started with the development of a CEP-stabilized driving laser. We successfully constructed sub-10-

fs Ti:sapphire oscillators[112,113] and developed an optical frequency comb using f–$2f$ and f–0 interferometry.[114,115] The CEP-stabilized seed pulses were amplified to a high energy and then spectrally broadened and compressed to 3.8 fs using a differentially pumped gas-filled hollow-core fiber[116,117] or solid thin plates[118] and chirped mirrors as the compressor. The CEP of the amplified pulse was stabilized using f–$2f$ spectral interferometry, and the feedback signal was used to control the displacement of a prism in the laser compressor to realize CEP stabilization with fluctuations of < 200 mrad for single shot measurements.[119–121] With the CEP-controlled sub-5-fs driving laser, we performed studies on HHG and obtained the HHG spectra as a function of the CEP and pulse duration,[122–124] as shown in Fig. 7.

On the basis of the development of the CEP-stabilized sub-5-fs laser, the first attosecond beamline at the Institute of Physics, Chinese Academy of Sciences (IOP-CAS) was constructed in 2010, as shown in Fig. 8.

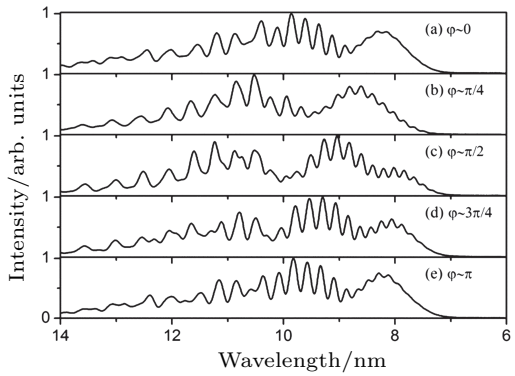

Fig. 7. (color online) High-order harmonic spectrum dependence on the CEP. XUV spectra for the CEPs of $\varphi = 0$, $\varphi = \pi/4$, $\varphi = \pi/2$, $\varphi = 3\pi/4$, $\varphi = \pi$ are shown in panels (a)–(e), respectively. Adapted from Ref. [121].

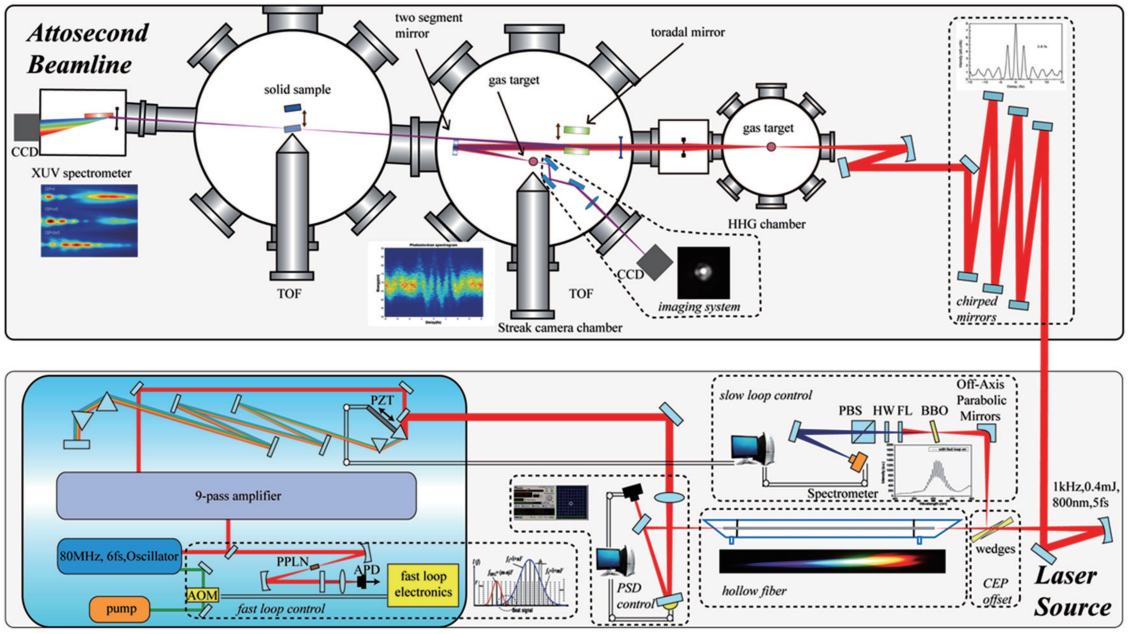

Fig. 8. (color online) Schematic of the existing attosecond beamline at IOP-CAS.

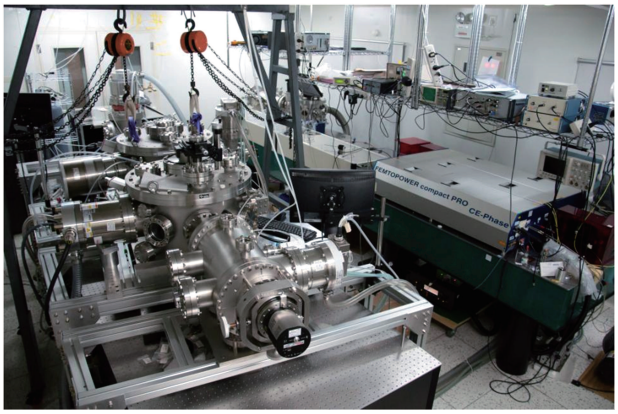

Fig. 9. (color online) Photograph of the existing attosecond beamline at IOP-CAS.

The driving laser pulse was sub-5-fs with energy of 0.4 mJ, and the CEP fluctuation was < 200 mrad for single shot measurement, as described above. The vacuum system of the attosecond beamline is composed of an HHG chamber, a streaking camera chamber, an application chamber, and an XUV flat-field spectrometer. A photograph of the beamline is shown in Fig. 9.

Using the attosecond beamline, we performed the generation and characterization of single attosecond XUV pulses, attosecond time-resolved measurements, and attosecond transient absorption experiments. The first attosecond streaking trace was successfully recorded in 2012, as shown in Fig. 10.

The retrieved single attosecond pulse duration is 160 as at 82 eV, as shown in Fig. 10(c),[125–127] and the e-field of the IR pulse is reconstructed as shown in Fig. 11.

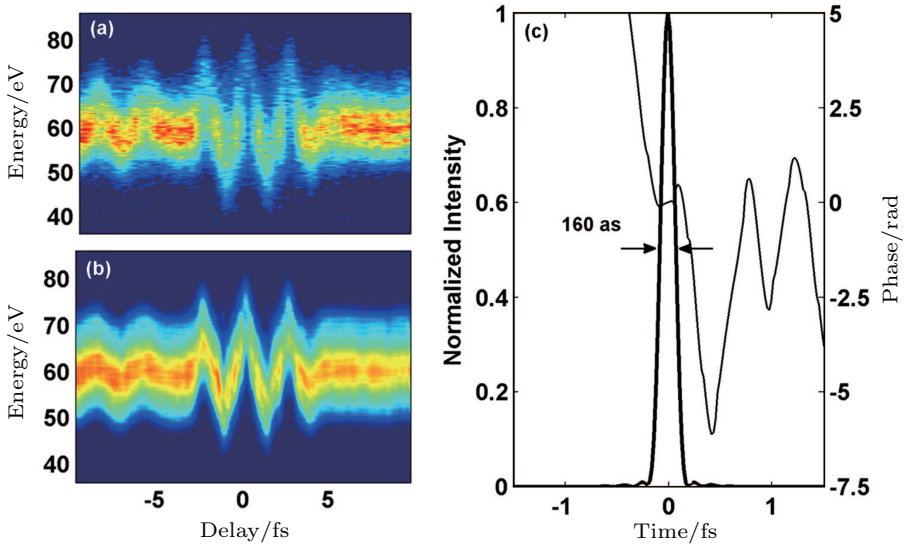

Fig. 10. (color online) (a) Attosecond streaking trace composed of photoelectrons from a Ne target as a function of the delay between the XUV and IR pulses, (b) FROG-CRAB reconstruction, and (c) the retrieved temporal amplitude and phase of the attosecond pulse. Adapted from Ref. [125].

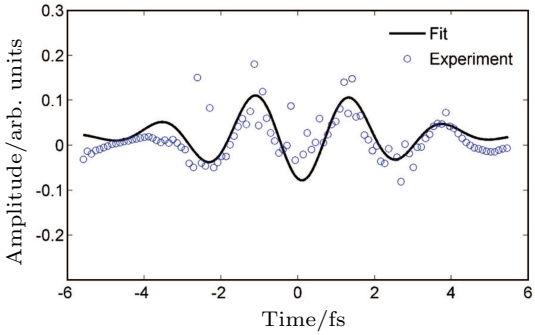

Fig. 11. (color online) The e-field of the femtosecond IR pulse reconstructed from the attosecond streaking spectrogram. Adapted from Ref. [125].

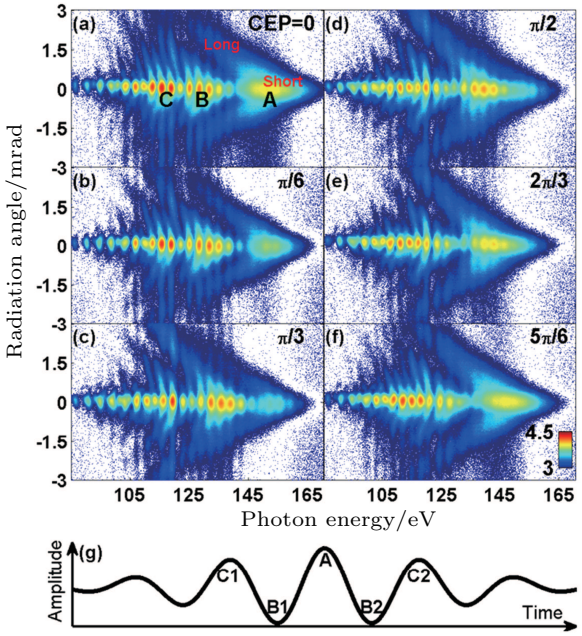

Fig. 12. (color online) (a)–(f) Experimental arrow-like high-order harmonic spectra with different CEPs. (g) Schematic of the driven laser field when CEP = 0. All the colorbars are the same as in (f), on a log scale. Adapted from Ref. [128].

Using the established attosecond beamline, we performed studies on full quantum resolved trajectories in HHG, as shown in Fig. 12. The short and long trajectories were clearly resolved in space and time.[128] The results elucidate the dynamics of the ionization and recombination for the generation of XUV radiation.

4. Conclusion and perspectives

To overcome the limitations of the current beamlines reported in the literature, the four XUV beamlines in the ALS are designed specifically for applications to study the ultrafast dynamics in atoms, molecules, and condensed matter. The purpose of integrating attosecond broadband XUV pulses and femtosecond narrowband XUV pulses with e-TOF, ARPES, COLTRIMS, PEEM, and XUV spectrometers is to develop one of the most sophisticated platforms that will enable versatile attosecond to femtosecond time-resolved measurements of ultrafast processes in matter with momentum and spatial resolutions simultaneously and allow researchers to probe and control microscopic ultrafast electron dynamics in atoms, molecules, surfaces, and bulk solid-state materials. This will eventually pave the way for comprehension and applications of related macroscopic phenomena covering multiple research disciplines in physics, chemistry, and biology.

Acknowledgments

The authors would like to thank Hainian Han, Jiangfeng Zhu, Qiang Du, Chenxia Yun, Wei Zhang, Peng Ye, Lifeng Wang, Minjie Zhan, Peng He, Yangyang Liu for the earlier contribution for the first attosecond beamline in the laboratory. The relevant researches have been partly supported by NSFC, MOST, and Chinese Academy of Sciences.

References

[1] Krausz F 2001 *Phys. World* **14** 41
[2] Krausz F and Ivanov M 2009 *Rev. Mod. Phys.* **81** 163
[3] Brabec T and Krausz F 2000 *Rev. Mod. Phys.* **72** 545
[4] Zewail A H 2000 *J. Phys. Chem. A* **104** 5660
[5] Bucksbaum P H 2007 *Science* **317** 766
[6] Drescher M, Hentschel M, Kienberger R, Tempea G, Spielmann C, Reider G A, Corkum P B and Krausz F 2001 *Science* **291** 1923
[7] Bucksbaum P H 2003 *Nature* **421** 593
[8] Corkum P B 1993 *Phys. Rev. Lett.* **71** 1994
[9] Hentschel M, Kienberger R, Spielmann C, Reider G A, Milosevic N, Brabec T, Corkum P, Heinzmann U, Drescher M and Krausz F 2001 *Nature* **414** 509
[10] Chang Z H, Corkum P B and Leone S R 2016 *J. Opt. Soc. Am. B-Opt. Phys.* **33** 1081
[11] Chini M, Zhao K and Chang Z H 2014 *Nat. Photon.* **8** 178
[12] Baltuska A, Udem T, Uiberacker M, Hentschel M, Goulielmakis E, Gohle C, Holzwarth R, Yakovlev V S, Scrinzi A, Hansch T W and Krausz F 2003 *Nature* **421** 611
[13] Goulielmakis E, Schultze M, Hofstetter M, Yakovlev V S, Gagnon J, Uiberacker M, Aquila A L, Gullikson E M, Attwood D T, Kienberger R, Krausz F and Kleineberg U 2008 *Science* **320** 1614
[14] Corkum P B, Burnett N H and Ivanov M Y 1994 *Opt. Lett.* **19** 1870
[15] Sansone G, Benedetti E, Calegari F, Vozzi C, Avaldi L, Flammini R, Poletto L, Villoresi P, Altucci C, Velotta R, Stagira S, De Silvestri S and Nisoli M 2006 *Science* **314** 443
[16] Ferrari F, Calegari F, Lucchini M, Vozzi C, Stagira S, Sansone G and Nisoli M 2010 *Nat. Photon.* **4** 875
[17] Abel M J, Pfeifer T, Nagel P M, Boutu W, Bell M J, Steiner C P, Neumark D M and Leone S R 2009 *Chem. Phys.* **366** 9
[18] Mashiko H, Gilbertson S, Chini M, Feng X M, Yun C X, Wang H, Khan S D, Chen S Y and Chang Z H 2009 *Opt. Lett.* **34** 3337
[19] Feng X M, Gilbertson S, Mashiko H, Wang H, Khan S D, Chini M, Wu Y, Zhao K and Chang Z H 2009 *Phys. Rev. Lett.* **103** 183901
[20] Zhao K, Zhang Q, Chini M, Wu Y, Wang X W and Chang Z H 2012 *Opt. Lett.* **37** 3891
[21] Kim K T, Zhang C M, Ruchon T, Hergott J F, Auguste T, Villeneuve D M, Corkum P B and Quere F 2013 *Nat. Photon.* **7** 651
[22] Quere F, Vincenti H, Borot A, Monchoce S, Hammond T J, Kim K T, Wheeler J A, Zhang C M, Ruchon T, Auguste T, Hergott J F, Villeneuve D M, Corkum P B and Lopez-Martens R 2014 *J. Phys. B-At. Mol. Opt. Phys.* **47** 124004
[23] Chang Z H, Rundquist A, Wang H W, Murnane M M and Kapteyn H C 1997 *Phys. Rev. Lett.* **79** 2967
[24] Shan B and Chang Z H 2001 *Phys. Rev. A* **65** 011804
[25] Li J, Ren X M, Yin Y C, Zhao K, Chew A, Cheng Y, Cunningham E, Wang Y, Hu S Y, Wu Y, Chini M and Chang Z H 2017 *Nat. Commun.* **8** 794
[26] Ren X M, Li J, Yin Y C, Zhao K, Chew A, Wang Y, Hu S Y, Cheng Y, Cunningham E, Wu Y, Chini M and Chang Z H 2018 *J. Opt.* **20** 023001
[27] Gaumnitz T, Jain A, Pertot Y, Huppert M, Jordan I, Ardana-Lamas F and Wörner H J 2017 *Opt. Express* **25** 27506
[28] Takahashi E J, Lan P F, Mücke O D, Nabekawa Y and Midorikawa K 2013 *Nat. Commun.* **4** 2691
[29] Hammond T J, Brown G G, Kim K T, Villeneuve D M and Corkum P B 2016 *Nat. Photon.* **10** 171
[30] Frank F, Arrell C, Witting T, Okell W A, McKenna J, Robinson J S, Haworth C A, Austin D, Teng H, Walmsley I A, Marangos J P and Tisch J W G 2012 *Rev. Sci. Instrum.* **83** 071101
[31] Itatani J, Quere F, Yudin G L, Ivanov M Y, Krausz F and Corkum P B 2002 *Phys. Rev. Lett.* **88** 173903
[32] Frank F, Arrell C, Witting T, Okell W A, McKenna J, Robinson J S, Haworth C A, Austin D, Teng H, Walmsley I A, Marangos J P and Tisch J W G 2012 *Rev. Sci. Instrum.* **83** 071101
[33] Mairesse Y and Quere F 2005 *Phys. Rev. A* **71** 011401
[34] Chini M, Gilbertson S, Khan S D and Chang Z H 2010 *Opt. Express* **18** 13006
[35] Kienberger R, Goulielmakis E, Uiberacker M, Baltuska A, Yakovlev V, Bammer F, Scrinzi A, Westerwalbesloh T, Kleineberg U, Heinzmann U, Drescher M and Krausz F 2004 *Nature* **427** 817
[36] Mathies R A, Cruz C H B, Pollard W T and Shank C V 1988 *Science* **240** 777
[37] Loh Z H and Leone S R 2008 *J. Chem. Phys.* **128** 204302
[38] Beck A R, Neumark D M and Leone S R 2015 *Chem. Phys. Lett.* **624** 119
[39] Drescher M, Hentschel M, Kienberger R, Uiberacker M, Yakovlev V, Scrinzi A, Westerwalbesloh T, Kleineberg U, Heinzmann U and Krausz F 2002 *Nature* **419** 803
[40] Schultze M, Fiess M, Karpowicz N, Gagnon J, Korbman M, Hofstetter M, Neppl S, Cavalieri A L, Komninos Y, Mercouris T, Nicolaides C A, Pazourek R, Nagele S, Feist J, Burgdorfer J, Azzeer A M, Ernstorfer R, Kienberger R, Kleineberg U, Goulielmakis E, Krausz F and Yakovlev V S 2010 *Science* **328** 1658
[41] Ossiander M, Siegrist F, Shirvanyan V, Pazourek R, Sommer A, Latka T, Guggenmos A, Nagele S, Feist J, Burgdörfer J, Kienberger R and Schultze M 2016 *Nat. Phys.* **13** 280
[42] Neppl S, Ernstorfer R, Cavalieri A L, Lemell C, Wachter G, Magerl E, Bothschafter E M, Jobst M, Hofstetter M, Kleineberg U, Barth J V, Menzel D, Burgdörfer J, Feulner P, Krausz F and Kienberger R 2015 *Nature* **517** 342
[43] Förg B, Schötz J, Süßmann F, Förster M, Krüger M, Ahn B, Okell W A, Wintersperger K, Zherebtsov S, Guggenmos A, Pervak V, Kessel A, Trushin S A, Azzeer A M, Stockman M I, Kim D, Krausz F, Hommelhoff P and Kling M F 2016 *Nat. Commun.* **7** 11717
[44] Sansone G, Kelkensberg F, Perez-Torres J F, Morales F, Kling M F, Siu W, Ghafur O, Johnsson P, Swoboda M, Benedetti E, Ferrari F, Lepine F, Sanz-Vicario J L, Zherebtsov S, Znakovskaya I, L'Huillier A, Ivanov M Y, Nisoli M, Martin F and Vrakking M J J 2010 *Nature* **465** 763
[45] Cavalieri A L, Muller N, Uphues T, Yakovlev V S, Baltuska A, Horvath B, Schmidt B, Blumel L, Holzwarth R, Hendel S, Drescher M, Kleineberg U, Echenique P M, Kienberger R, Krausz F and Heinzmann U 2007 *Nature* **449** 1029
[46] Schiffrin A, Paasch-Colberg T, Karpowicz N, Apalkov V, Gerster D, Muhlbrandt S, Korbman M, Reichert J, Schultze M, Holzner S, Barth J V, Kienberger R, Ernstorfer R, Yakovlev V S, Stockman M I and Krausz F 2012 *Nature* **493** 70
[47] Schultze M, Bothschafter E M, Sommer A, Holzner S, Schweinberger W, Fiess M, Hofstetter M, Kienberger R, Apalkov V, Yakovlev V S, Stockman M I and Krausz F 2012 *Nature* **493** 75
[48] Neppl S, Ernstorfer R, Cavalieri A L, Lemell C, Wachter G, Magerl E, Bothschafter E M, Jobst M, Hofstetter M, Kleineberg U, Barth J V, Menzel D, Burgdorfer J, Feulner P, Krausz F and Kienberger R 2015 *Nature* **517** 342
[49] Ossiander M, Siegrist F, Shirvanyan V, Pazourek R, Sommer A, Latka T, Guggenmos A, Nagele S, Feist J, Burgdorfer J, Kienberger R and Schultze M 2016 *Nat. Phys.* **13** 280
[50] Wang H, Chini M, Chen S Y, Zhang C H, He F, Cheng Y, Wu Y, Thumm U and Chang Z H 2010 *Phys. Rev. Lett.* **105** 143002
[51] Goulielmakis E, Loh Z H, Wirth A, Santra R, Rohringer N, Yakovlev V S, Zherebtsov S, Pfeifer T, Azzeer A M, Kling M F, Leone S R and Krausz F 2010 *Nature* **466** 739
[52] Kevan S D 1992 *Angle-resolved Photoemission: Theory and Current Applications* (Amesterdan: Elsevier)
[53] Damascelli A, Hussain Z and Shen Z X 2003 *Rev. Mod. Phys.* **75** 473
[54] Wlegmann L 1972 *J. Microscopy* **96** 1
[55] Bauer E 1994 *Rep. Prog. Phys.* **57** 895
[56] Ullrich J, Moshammer R, Dorner R, Jagutzki O, Mergel V, Schmidt-Bocking H and Spielberger L 1997 *J. Phys. B-At. Mol. Opt. Phys.* **30** 2917
[57] Dorner R, Mergel V, Jagutzki O, Spielberger L, Ullrich J, Moshammer R and Schmidt-Bocking H 2000 *Phys. Rep.-Rev. Sec. Phys. Lett.* **330** 95
[58] Reinert F and Hufner S 2005 *New J. Phys.* **7** 97
[59] Mathias S, Miaja-Avila L, Murnane M M, Kapteyn H, Aeschlimann M and Bauer M 2007 *Rev. Sci. Instrum.* **78** 083105
[60] Eich S, Stange A, Carr A V, Urbancic J, Popmintchev T, Wiesenmayer M, Jansen K, Ruffing A, Jakobs S, Rohwer T, Hellmann S, Chen C, Matyba P, Kipp L, Rossnagel K, Bauer M, Murnane M M, Kapteyn H C, Mathias S and Aeschlimann M 2014 *J. Electron. Spectrosc. Relat. Phenom.* **195** 231

[61] Froud C A, Bonora S, Springate E, Langley A J, Wolff D S, Blake S P, Brummitt P A, Cavalleri A, Dhesi S, Poletto L, Villoresi P, Marangos J P, Tisch J W G, Seddon E, Hirst G J, Underwood J, Fielding H H, McCoustra M, Turcu E and Collier J L *Central Laser Facility Annual Report* 2007/2008 pp. 240–242

[62] Turcu I C E, Springate E, Froud C A, Cacho C M, Collier J L, Bryan W A, Nemeth G, Marangos J P, Tisch J W G, Torres R, Siegel T, Brugnera L, Underwood J G, Procino I, Newell W R, Altucci C, Velotta R, King R B, Alexander J D, Calvert C R, Kelly O, Greenwood J B, Williams I D, Cavalleri A, Petersen J C, Dean N, Dhesi S S, Poletto L, Villoresi P, Frassetto F, Bonora S and Roper M D 2010 *Proc. SPIE* **7469** 746902

[63] Petersen J C, Kaiser S, Dean N, Simoncig A, Liu H Y, Cavalieri A L, Cacho C, Turcu I C E, Springate E, Frassetto F, Poletto L, Dhesi S S, Berger H and Cavalleri A 2011 *Phys. Rev. Lett.* **107** 177402

[64] Gierz I, Petersen J C, Mitrano M, Cacho C, Turcu I C E, Springate E, Stohr A, Kohler A, Starke U and Cavalleri A 2013 *Nat. Mater.* **12** 1119

[65] Ulstrup S, Johannsen J C, Cilento F, Miwa J A, Crepaldi A, Zacchigna M, Cacho C, Chapman R, Springate E, Mammadov S, Fromm F, Raidel C, Seyller T, Parmigiani F, Grioni M, King P D C and Hofmann P 2014 *Phys. Rev. Lett.* **112** 257401

[66] Johannsen J C, Ulstrup S, Crepaldi A, Cilento F, Zacchigna M, Miwa J A, Cacho C, Chapman R T, Springate E, Fromm F, Raidel C, Seyller T, King P D C, Parmigiani F, Grioni M and Hofmann P 2015 *Nano Lett.* **15** 326

[67] Cilento F, Manzoni G, Sterzi A, Peli S, Ronchi A, Crepaldi A, Boschini F, Cacho C, Chapman R, Springate E, Eisaki H, Greven M, Berciu M, Kemper A F, Damascelli A, Capone M, Giannetti C and Parmigiani F 2018 *Sci. Adv.* **4** eaar1998

[68] Frietsch B, Carley R, Dobrich K, Gahl C, Teichmann M, Schwarzkopf O, Wernet P and Weinelt M 2013 *Rev. Sci. Instrum.* **84** 075106

[69] Frietsch B, Bowlan J, Carley R, Teichmann M, Wienholdt S, Hinzke D, Nowak U, Carva K, Oppeneer P M and Weinelt M 2015 *Nat. Commun.* **6** 8262

[70] Locher R, Lucchini M, Herrmann J, Sabbar M, Weger M, Ludwig A, Castiglioni L, Greif M, Hengsberger M, Gallmann L and Keller U 2014 *Rev. Sci. Instrum.* **85** 013113

[71] Magerl E, Neppl S, Cavalieri A L, Bothschafter E M, Stanislawski M, Uphues T, Hofstetter M, Kleineberg U, Barth J V, Menzel D, Krausz F, Ernstorfer R, Kienberger R and Feulner P 2011 *Rev. Sci. Instrum.* **82** 063104

[72] Dakovski G L, Li Y, Durakiewicz T and Rodriguez G 2010 *Rev. Sci. Instrum.* **81** 073108

[73] Plogmaker S, Terschlusen J A, Krebs N, Svanqvist M, Forsberg J, Cappel U B, Rubensson J E, Siegbahn H and Soderstrom J 2015 *Rev. Sci. Instrum.* **86** 123107

[74] Grazioli C, Callegari C, Ciavardini A, Coreno M, Frassetto F, Gauthier D, Golob D, Ivanov R, Kivimaki A, Mahieu B, Bucar B, Merhar M, Miotti P, Poletto L, Polo E, Ressel B, Spezzani C and De Ninno G 2014 *Rev. Sci. Instrum.* **85** 023104

[75] Eckle P, Smolarski M, Schlup P, Biegert J, Staudte A, Schoffler M, Muller H G, Dorner R and Keller U 2008 *Nat. Phys.* **4** 565

[76] Eckle P, Pfeiffer A N, Cirelli C, Staudte A, Dorner R, Muller H G, Buttiker M and Keller U 2008 *Science* **322** 1525

[77] Pfeiffer A N, Cirelli C, Smolarski M, Dimitrovski D, Abu-Samha M, Madsen L B and Keller U 2012 *Nat. Phys.* **8** 76

[78] Pfeiffer A N, Cirelli C, Smolarski M, Dorner R and Keller U 2011 *Nat. Phys.* **7** 428

[79] Pfeiffer A N, Cirelli C, Smolarski M, Wang X, Eberly J H, Dorner R and Keller U 2011 *New J. Phys.* **13** 093008

[80] Zhang W B, Li Z C, Lu P F, Gong X C, Song Q Y, Ji Q Y, Lin K, Ma J Y, He F, Zeng H P and Wu J 2016 *Phys. Rev. Lett.* **117** 103002

[81] Quan W, Hao X L, Hu X Q, Sun R P, Wang Y L, Chen Y J, Yu S G, Xu S P, Xiao Z L, Lai X Y, Li X Y, Becker W, Wu Y, Wang J G, Liu X J and Chen J 2017 *Phys. Rev. Lett.* **119** 243203

[82] Sun X F, Li M, Ye D F, Xin G G, Fu L B, Xie X G, Deng Y K, Wu C Y, Liu J, Gong Q H and Liu Y Q 2014 *Phys. Rev. Lett.* **113** 103001

[83] Ma X W, Zhu X L, Liu H P, Li B, Zhang S F, Cao S P, Feng W T and Xu S Y 2008 *Sci. Chin. Ser. G: Phys. Mech. Astron.* **51** 755

[84] Gagnon E, Sandhu A S, Paul A, Hagen K, Czasch A, Jahnke T, Ranitovic P, Cocke C L, Walker B, Murnane M M and Kapteyn H C 2008 *Rev. Sci. Instrum.* **79** 063102

[85] Gagnon E, Ranitovic P, Tong X M, Cocke C L, Murnane M M, Kapteyn H C and Sandhu A S 2007 *Science* **317** 1374

[86] Rietz H, Gopal R, Sperl A G, Simeonidis K and Ullrich J 2009 *J. Phys.: Conf. Ser.* **194** 142016

[87] Cao W, De S, Singh K P, Chen S, Schoffler M S, Alnaser A S, Bocharova I A, Laurent G, Ray D, Zherebtsov S, Kling M F, Ben-Itzhak I, Litvinyuk I V, Belkacem A, Osipov T, Rescigno T and Cocke C L 2010 *Phys. Rev. A* **82** 043410

[88] Cao W, Laurent G, De S, Schoffler M, Jahnke T, Alnaser A S, Bocharova I A, Stuck C, Ray D, Kling M F, Ben-Itzhak I, Weber T, Landers A L, Belkacem A, Dorner R, Orel A E, Rescigno T N and Cocke C L 2011 *Phys. Rev. A* **84** 053406

[89] Cao W, Laurent G, Jin C, Li H, Wang Z, Lin C D, Ben-Itzhak I and Cocke C L 2012 *J. Phys. B-At. Mol. Opt. Phys.* **45** 074013

[90] Weber S J, Manschwetus B, Billon M, Bottcher M, Bougeard M, Breger P, Geleoc M, Gruson V, Huetz A, Lin N, Picard Y J, Ruchon T, Salieres P and Carre B 2015 *Rev. Sci. Instrum.* **86** 033108

[91] Sabbar M, Heuser S, Boge R, Lucchini M, Gallmann L, Cirelli C and Keller U 2014 *Rev. Sci. Instrum.* **85** 103113

[92] Cirelli C, Sabbar M, Heuser S, Boge R, Lucchini M, Gallmann L and Keller U 2015 *IEEE J. Sel. Top. Quantum Electron.* **21** 8700307

[93] Sabbar M, Heuser S, Boge R, Lucchini M, Carette T, Lindroth E, Gallmann L, Cirelli C and Keller U 2015 *Phys. Rev. Lett.* **115** 133001

[94] Heringdorf F M Z, Chelaru L I, Mollenbeck S, Thien D and Hoegen M H V 2007 *Surf. Sci.* **601** 4700

[95] Stockman M I, Kling M F, Kleineberg U and Krausz F 2007 *Nat. Photon.* **1** 539

[96] Mikkelsen A, Schwenke J, Fordell T, Luo G, Klunder K, Hilner E, Anttu N, Zakharov A A, Lundgren E, Mauritsson J, Andersen J N, Xu H Q and L'Huillier A 2009 *Rev. Sci. Instrum.* **80** 123703

[97] Marsell E, Arnold C L, Lorek E, Guenot D, Fordell T, Miranda M, Mauritsson J, Xu H X, L'Huillier A and Mikkelsen A 2013 *Ann. Phys.-Berlin* **525** 162

[98] Lin J Q, Weber N, Wirth A, Chew S H, Escher M, Merkel M, Kling M F, Stockman M I, Krausz F and Kleineberg U 2009 *J. Phys.: Condes. Matter* **21** 314005

[99] Chew S H, Sussmann F, Spath C, Wirth A, Schmidt J, Zherebtsov S, Guggenmos A, Oelsner A, Weber N, Kapaldo J, Gliserin A, Stockman M I, Kling M F and Kleineberg U 2012 *Appl. Phys. Lett.* **100** 051904

[100] Hommelhoff P and Kling M F 2015 *Attosecond NanoPhys.: From Basic Sci. Appl.* pp. 281–324

[101] Schmidt J, Guggenmos A, Chew S H, Gliserin A, Hogner M, Kling M F, Zou J, Spath C and Kleineberg U 2017 *Rev. Sci. Instrum.* **88** 083105

[102] Kuhn S, Dumergue M, Kahaly S, Mondal S, Fule M, Csizmadia T, Farkas B, Major B, Varallyay Z, Calegari F, Devetta M, Frassetto F, Mansson E, Poletto L, Stagira S, Vozzi C, Nisoli M, Rudawski P, Maclot S, Campi F, Wikmark H, Arnold C L, Heyl C M, Johnsson P, L'Huillier A, Lopez-Martens R, Haessler S, Bocoum M, Boehle F, Vernier A, Iaquaniello G, Skantzakis E, Papadakis N, Kalpouzos C, Tzallas P, Lepine F, Charalambidis D, Varju K, Osvay K and Sansone G 2017 *J. Phys. B-At. Mol. Opt. Phys.* **50** 132002

[103] Frassetto F, Cacho C, Froud C A, Turcu I C E, Villoresi P, Bryan W A, Springate E and Poletto L 2011 *Opt. Express* **19** 19169

[104] Emma P, Akre R, Arthur J, Bionta R, Bostedt C, Bozek J, Brachmann A, Bucksbaum P, Coffee R, Decker F J, Ding Y, Dowell D, Edstrom S, Fisher A, Frisch J, Gilevich S, Hastings J, Hays G, Hering Ph, Huang Z, Iverson R, Loos H, Messerschmidt M, Miahnahri A, Moeller S, Nuhn H D, Pile G, Ratner D, Rzepiela J, Schultz D, Smith T, Stefan P, Tompkins H, Turner J, Welch J, White W, Wu J, Yocky G and Galayda J 2010 *Nat. Photon.* **4** 641

[105] Xue L, Reininger R, Wu Y Q, Zou Y, Xu Z M, Shi Y B, Dong J, Ding H, Sun J L, Wang Y and Tai R Z 2014 *J. Synchrotron Rad.* **21** 273

[106] Ackermann W 2007 *Nat. Photon.* **1** 336

[107] Feldhaus J, Krikunova M, Meyer M, Möller Th, Moshammer R, Rudenko A, Tschentscher Th and Ullrich J 2013 *J. Phys. B: At. Mol. Opt. Phys.* **46** 164002

[108] Allaria E 2012 *Nat. Photon.* **6** 699

[109] Li C Y, Wei S, Du X W, Du L L, Wang Q P, Zhang W Q, Wu G R, Dai D X and Yang X M 2015 *Nucl. Instr. Meth. A* **783** 65

[110] Poletto L and Frassetto F 2010 *Appl. Opt.* **49** 5465

[111] Poletto L and Frassetto F 2013 *Appl. Sci.-Basel* **3** 1

[112] Zhao Y Y, Wang P, Zhang W, Tian J R and Wei Z Y 2007 *Sci. Chin.-Phys. Mech. & Astron.* **50** 261

[113] Zhang Q, Zhao Y Y and Wei Z Y 2009 *Chin. Phys. Lett.* **26** 044208

[114] Han H N, Z Y Y, Zhang W, Zhu J F, Wang P, Wei Z Y and Li S Q 2007 *Acta Phys. Sin.* **56** 2756 (in Chinese)

[115] Han H N, Zhang W, Tong J J, Wang Y H, Wang P, Wei Z Y, Li D H, Shen N C, Nie Y X and Dong T Q 2007 *Acta Phys. Sin.* **56** 291 (in Chinese)

[116] Zhu J F, Wang P, Han H N, Teng H and Wei Z Y 2008 *Sci. Chin.* **51** 507

[117] Zhang W, Teng H, Yun C X, Zhong X, Hou X and Wei Z Y 2010 *Chin. Phys. Lett.* **27** 054211

[118] He P, Liu Y Y, Zhao K, Teng H, He X K, Huang P, Huang H D, Zhong S Y, Jiang Y J, Fang S B, Hou X and Wei Z Y 2017 *Opt. Lett.* **42** 474

[119] Zhu J F, Du Q, Wang X W L, Teng H, Han H N, Wei Z Y and Hou X 2008 *Acta Phys. Sin.* **57** 7753 (in Chinese)

[120] Du Q, Zhu J, Teng H, Yun C X and Wei Z Y 2008 *Chin. Sci. Bull.* **53** 671

[121] Zhang W, Teng H, Yun C X, Ye P, Zhan M J, Zhong S Y, He X K, Wang L F and Wei Z Y 2014 *Chin. Phys. Lett.* **31** 084204

[122] Yun C X, Teng H, Zhang W, Zhan M J, Han H N, Zhong X, Wei Z Y, Wang B B and Hou X 2010 *Chin. Phys. B* ***19*** *124210*

[123] Teng H, Yun C X, He X K, Zhang W, Wang L F, Zhan M J, Wang B B and Wei Z Y 2011 *Opt. Express* **19** 17408

[124] Teng H, Yun C X, Zhu J F, Han H N, Zhong X, Zhang W, Hou X and Wei Z Y 2009 *Chin. Phys. Lett.* **26** 113201

[125] Zhan M J, Ye P, Teng H, He X K, Zhang W, Zhong S Y, Wang L F, Yun C X and Wei Z Y 2013 *Chin. Phys. Lett.* **30** 093201

[126] Zhong S Y, He X K, Ye P, Zhan M J, Teng H and Wei Z Y 2013 *Opt. Express* **21** 17498

[127] Ye P, Teng H, He X k, Zhong S Y, Wang L F, Zhan M J, Zhang W, Yun C X and Wei Z Y 2014 *Phys. Rev. A* **90** 063808

[128] Ye P, He X K, Teng H, Zhan M J, Zhong S Y, Zhang W, Wang L F and Wei Z Y 2014 *Phys. Rev. Lett.* **113** 073601